Supplementary Information for

Effect of cholesterol on nanoparticle translocation across a lipid bilayer

Masaya Tajima, Hideya Nakamura,* Shuji Ohsaki and Satoru Watano

Department of Chemical Engineering, Osaka Metropolitan University,

1-1 Gakuen-cho, Naka-ku, Sakai, Osaka 599-8531, Japan

*Address correspondence to hideyanakamura@omu.ac.jp (H. Nakamura)

Contents

A. Supplementary Text

A.1 Experimental method

To verify the findings obtained from the MD simulations in the present study, the membrane-crossing of NP across cholesterol-containing lipid bilayer membranes was investigated experimentally. In this study, a planar bilayer lipid membrane (BLM) with the electrophysiological technique was used [1, 2]. This experimental technique can investigate the cell membrane-crossing of ions, molecules, and NPs under an electric field [1-5]. Materials and methods used in this study are presented in the following section. More details can be seen in our previous study [2].

The following reagents were used in the experiment: 1,2-dioleoyl-sn-glycero-3-phosphocholine (DOPC, Avanti Polar Lipids, 850375), 1,2-dioleoyl-sn-glycero-3-phosphate (DOPA, Avanti Polar

Lipids, 540875), cholesterol (47127-U, Merck), *n*-decane (040-21602, FUJIFILM Wako Pure Chemical), and KCl (169-03542, FUJIFILM Wako Pure Chemical). DOPC, DOPA, and cholesterol were dissolved into the *n*-decane at the same molar fraction as the simulation conditions, and a lipid/oil solution (10 mg/ml of all-lipids/*n*-decane) were prepared. For the NP, a cationic gold NP coated with 11-amino-1-undecanethiol (NP BS 003-075, ProChimia Surfaces) was used. The nominal particle diameter was 5.5 nm. The mean diameter and surface potential of the NP were 11.06 nm and 21.7 mV (in 154 mM KCl solution, the same as the simulation conditions). Characterization of the NP was conducted using a surface potential and particle size analyzer (Zetasizer Nano ZS, Malvern). The properties of the NP used in the experiment were very similar to the NP used in the MD simulation.

Fig. S1 shows experimental device and set-up. Planar BLMs were prepared by the droplet contact method (DCM) [1, 2, 5] as depicted in Fig. S1a. In a lipid/oil solution, an aqueous droplet covered with lipid monolayers were prepared. When the two droplets contacted each other, a BLM can be formed at the contact interface. A double-well device (Fig. S1b and S1c) was used to prepare a BLM. Details of the device were described in the literature [1, 2, 5]. Briefly, the BLM was formed at the through-hole fabricated between the two wells. Application of a transmembrane external electric field and the measurement of transmembrane current was performed through the Ag/AgCl electrodes fabricated at the bottom of the well. Fig. S1d shows the experimental setup, which was composed of the double-well device, recording electrode, patch-clamp amplifier, function generator, and personal computer for controlling and data recording. To measure transmembrane current through the BLM, the double-well device was connected to the multi-channel patch-clamp amplifier (Flex, Tecella). The patch-clamp amplifier was also connected to the function generator (FG110, Yokogawa Electric) for applying transmembrane voltage to the BLM. Ag/AgCl electrodes were connected to the recording electrode of the patch-clamp amplifier through a solderless breadboard (Fig. S1e). The double-well devices and patch-clamp amplifier were placed in a Faraday cage to minimize noise.

The experimental procedures were as follows. First, 1.2 μL of lipid/oil solution was dropped into each well. Second, 20 μL of KCl solution (154 mM) without NPs was dropped into each well. The two aqueous droplets contacted each other at the single through-hole, forming a BLM. To verify the quality of the formed BLM, the membrane resistance R_m and capacitance C_m were measured *in situ*. In the case of $R_m \geq 1$ GΩ and $C_m \geq 0.4$ μF/cm^2 [2], the BLM was considered to have passed the quality check and was used in the subsequent experiment. After that, 3.0 μL of solution dispersed with the

cationic gold NPs (2.0×10^{11} NPs/μL in 154 mM KCl) was injected into the aqueous droplet connected to the positive voltage side (left side droplet in Fig. S1a). 3.0 μL of solution without NPs (154 mM KCl only) was also injected into the aqueous droplet connected to the negative voltage side (right side droplet in Fig. S1a) to ensure the same volume in both droplets. Subsequently, a constant positive voltage was externally applied to the BLM for 60 min. After removing the applied voltage, the membrane resistance and capacitance were measured again. Finally, the aqueous droplets in both wells were sampled by pipetting, and their absorbance at 523.5 nm was measured using a microvolume spectrophotometer (Nano Drop, Thermo Fisher Scientific) to quantify the NP concentration in each droplet.

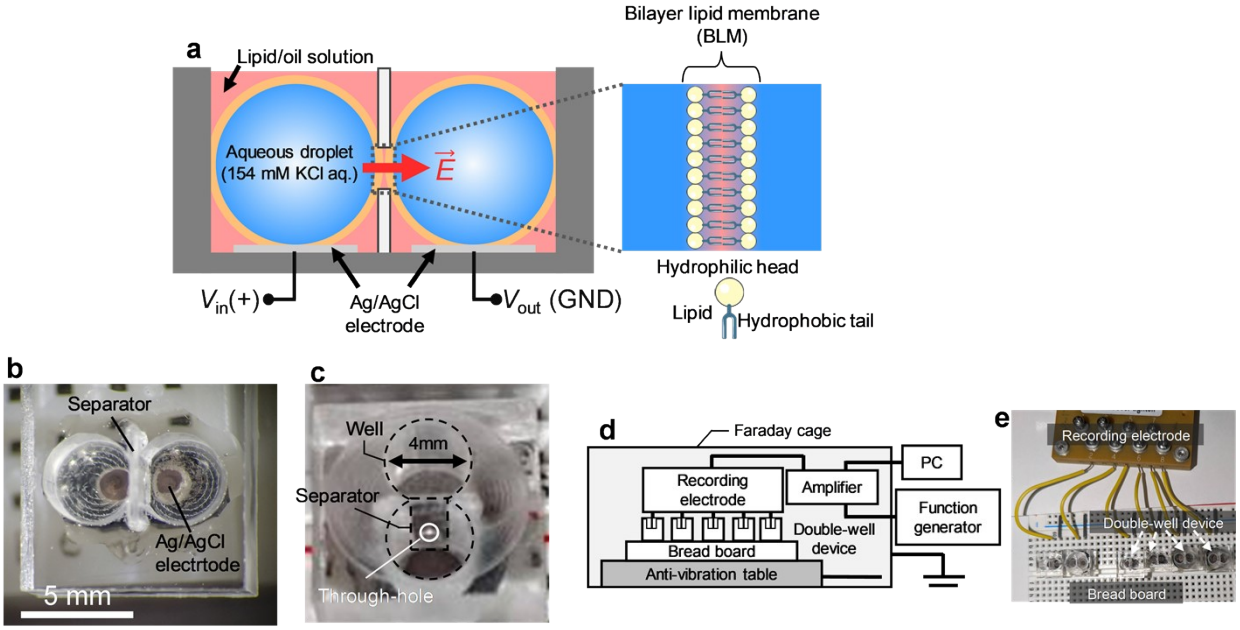

Fig. S1 (a) Planar bilayer lipid membrane (BLM) prepared by the droplet contact method (DCM). (b) Top view and (c) side view of the double-well device used in the experiment. (d) Experimental setup. (e) Double-well devices connected to solderless breadboard and recording electrode.

A.2. Comparison of the simulation results with the experimental results

Fig. S2a shows an experimental result, presenting a classification diagram of representative membrane and NP behaviors with respect to cholesterol content and applied membrane potential. The behaviors can be classified into the three modes, as was done with the MD simulation results. In the case of the experiment, the criteria for the three modes were defined as shown in Table S1. The mode of NP behavior with the highest occurrence probability among five independent experimental runs was

summarized, as was done with the MD simulation results. For comparison, Fig. S2b shows the simulation results presented in the main text (Fig. 5b in the main text).

The experimental results demonstrated qualitative agreement with the simulation results from the following viewpoints. First, the $\Delta\psi_{appl}$-criterion between mode I and II (or I and III) exhibited only slight variation as the cholesterol content increased. Second, the $\Delta\psi_{appl}$-window for mode II broadened at higher cholesterol contents (40 and 50 mol%). Therefore, the experimental results implied that the findings obtained from the MD simulation are valid. When we look at the experimental results in detail, some small inconsistencies were observed between the experimental and simulation results (ex., value of the $\Delta\psi_{appl,C}$ and transition of the modes of NP behavior with an increase in $\Delta\psi_{appl}$). We considered that this may be owing to difference between experimental and simulation systems and variability of the experimental data which is inherent in the experimental set-up. Nevertheless, the experimental results supported the findings obtained from the MD simulations in the present study.

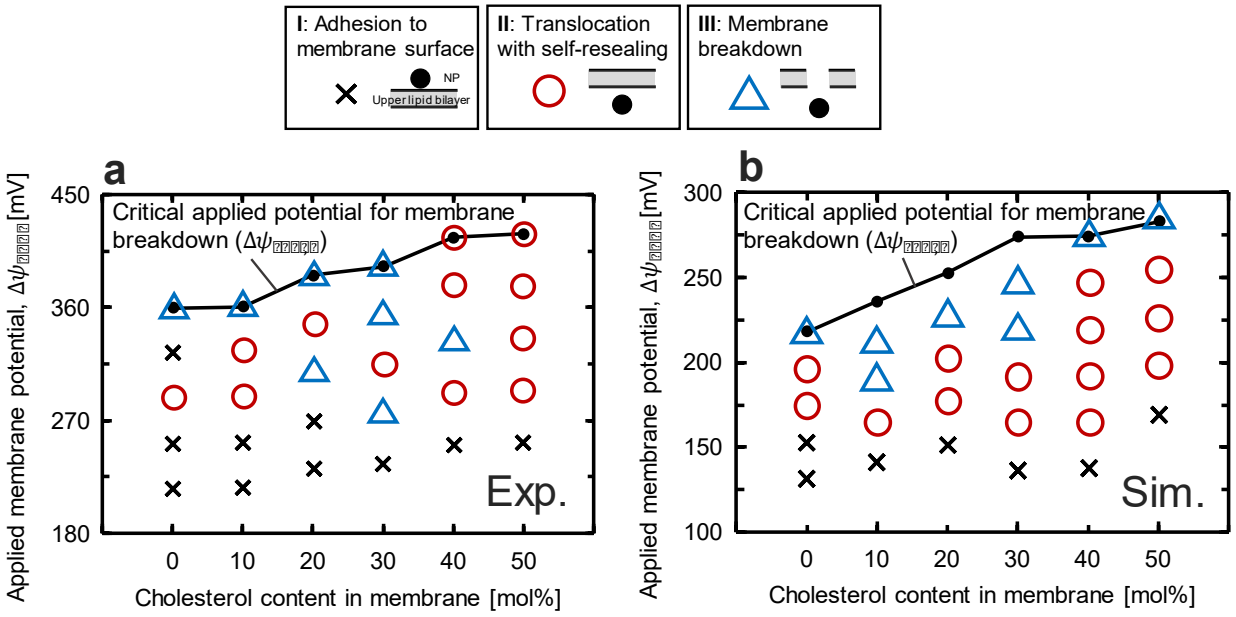

Fig. S2 Classification diagram of representative NP behavior with respect to cholesterol content and applied membrane potential, $\Delta\psi_{appl}$. (a) Experimental result and (b) simulation result. (b) is the same as Fig. 5b in the main text.

Table. S1 Criteria for the three modes of membrane and NP behaviors in the experiment. The criteria were defined according to R_m, C_m, and translocation ratio of NP. R_m and C_m are the membrane resistance and capacitance at the end of BLM experiment (after removing the applied voltage). The translocation ratio of NP was defined as $A_{PV}/(A_{PV}+A_G)$ [%], where A_{PV} and A_G are the absorbances of NP in the droplets connected to the positive voltage side and ground, respectively, at the end of BLM experiment.

Mode	Criteria for mode classification		Membrane crossing of NP	Membrane breakdown
	R_m and C_m	Translocation ratio of NP [-]		
I	$R_m \geq 1$ GΩ ∩ $C_m \geq 0.4$ μF/cm^2	0.0	No	No
II	$R_m \geq 1$ GΩ ∩ $C_m \geq 0.4$ μF/cm^2	>0.0	Yes	No
III	$R_m < 1$ GΩ ∪ $C_m < 0.4$ μF/cm^2	>0.0	Yes	Yes

A.3. Influence of the NP-membrane interaction events on the membrane lateral pressure

Fig. S3 shows the lateral membrane pressure in a system composed of cholesterol-containing membranes and solvents with NP under electric field. The vertical axis of Fig. S3 ($^{P_{ii,w/NP}}/\langle P_{ii}\rangle_{wo/NP}$) denotes the lateral pressure of membrane interacting with NP ($^{P_{ii,w/NP}}$) normalized by the time-averaged pressure of membrane without NP ($\langle P_{ii}\rangle_{wo/NP}$). The normalized value ($^{P_{ii,w/NP}}/\langle P_{ii}\rangle_{wo/NP}$) of 1.0 means that there is no effect of the interaction of NP with membrane on the membrane lateral pressure. As seen in Fig. S3, $^{P_{ii,w/NP}}/\langle P_{ii}\rangle_{wo/NP}$ exhibited a fluctuation around 1.0 and their average components were almost unchanged regardless of the time. Importantly, $^{P_{ii,w/NP}}/\langle P_{ii}\rangle_{wo/NP}$ did not change significantly even when the NP adhered to the membrane and translocated across the membrane (please see the regions with red and gray backgrounds). These results indicate that influence of the NP-membrane interaction events (adhesion, penetration, and translocation) on the membrane lateral pressure was almost negligible in the case of the present study.

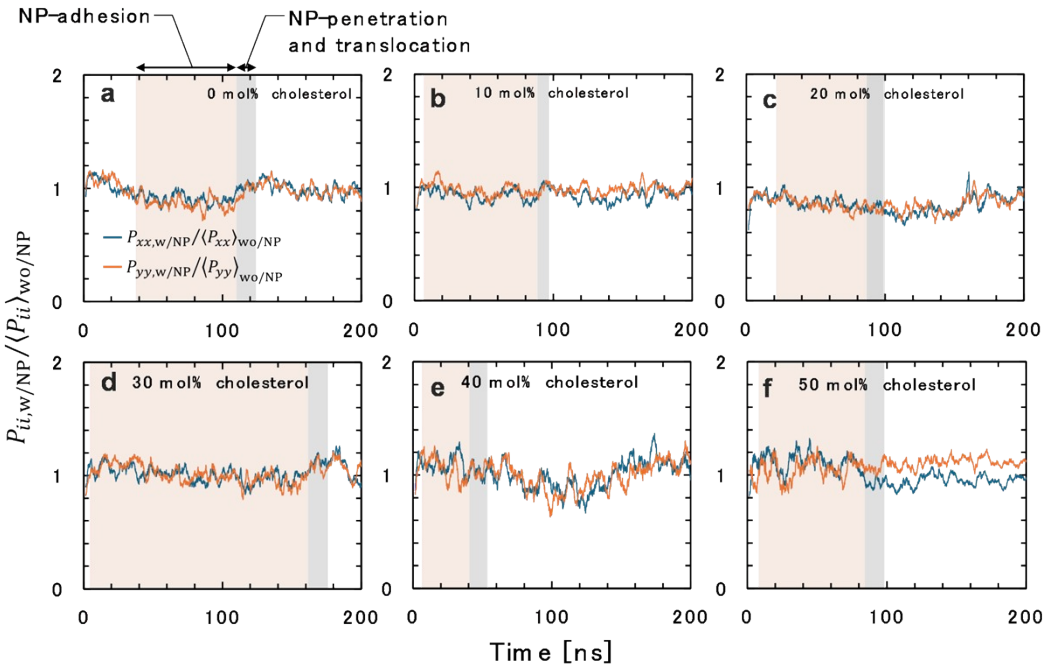

Fig. S3 Temporal change in the lateral pressure in a system composed of cholesterol-containing membranes, solvents, and NP under electric field. The region with a red background represents the duration during which NP adhered to the membrane. The region with a gray background represents the duration of NP translocation across the membrane with pore formation in the membrane. The vertical axis ($P_{ii,w/NP}/\langle P_{ii}\rangle_{wo/NP}$) denotes the lateral pressure of membrane interacting with NP normalized by the time-averaged pressure of membrane without NP. $P_{ii,w/NP}$ corresponds to the moving average of the raw data over 1.5 ns. The subscript w/NP denotes the simulation system with NP. All simulation results were obtained under the *NPzAT* ensemble. Applied membrane potential was 165 mV.

C. Supplementary References

1. R. Kawano, Y. Tsuji, K. Sato, T. Osaki, K. Kamiya, M. Hirano, T. Ide, N. Miki and S. Takeuchi, Automated Parallel Recordings of Topologically Identified Single Ion Channels, *Sci. Rep.*, 2013, **3**, 1995.
2. H. Nakamura, T. Okamura, M. Tajima, R. Kawano, M. Yamaji, S. Ohsaki and S. Watano, Enhancement of cell membrane permeability by using charged nanoparticles and a weak external electric field, *Phys. Chem. Chem. Phys.*, 2023, **25**, 32356–32363.
3. E. Rascol, J.-M. Devoisselle and joel c chopineau, The relevance of membrane models to

understand nanoparticles-cell membrane interactions, *Nanoscale*, 2016, **8**, 4780–4798.

4. L. Wu and X. Jiang, Recent developments in methodology employed to study the interactions between nanomaterials and model lipid membranes, *Anal. Bioanal. Chem.*, 2016, **408**, 2743–2758.
5. T. Kunthic, H. Watanabe, R. Kawano, Y. Tanaka, B. Promdonkoy, M. Yao and P. Boonserm, pH regulates pore formation of a protease activated Vip3Aa from Bacillus thuringiensis, *Biochim. Biophys. Acta - Biomembr.*, 2017, **1859**, 2234–2241.